RECENT OBSERVATIONS ON CAVITATION AND CAVITATION NOISE

C. E. Brennen and S. L. Ceccio
California Institute of Technology
Pasadena, California

ABSTRACT

This paper is primarily concerned with the acoustics of traveling bubble cavitation around foils or headforms. We begin with observations of individual bubbles and the acoustic signals they emit, our purpose being to identify areas of research which would enhance our understanding of the history of individual bubbles. Then we present some numerical integrations of the Rayleigh/Plesset equation for the same flows. The comparison is encouraging in terms of future synthesis of the noise by analytical means. Finally, bubble interaction effects which were omitted earlier are discussed and some recent analytical results including these effects are presented.

1. INTRODUCTION

Rather than attempting a comprehensive review of the state of knowledge of cavitation noise, this paper will focus on several issues where our understanding of the basic physical phenomena is, at best, quite limited. Our remarks will be confined to the noise generated by bubble cavitation and we will not attempt to deal with the added complications associated with fully or partially developed cavitation. The current state of knowledge of the noise generated by bubbly cavitation is thoroughly reviewed by Blake [1986] and well represented by the proceedings of the two previous symposiums in this series, so it may be more useful to focus on several key issues in order to identify areas which would benefit from further attention.

The most fundamental approach to cavitation noise begins with the nuclei population of the incoming stream. By constructing the dynamics and acoustics for each individual size of nucleus, one should in theory be able to combine this information with the nuclei number distribution to produce all the required information on cavitation noise levels and spectra. This, of course, assumes that bubbles do not interact acoustically or hydrodynamically. Such interactions will be considered in a later section. For present purposes, however, bubble interactions will be neglected.

Parenthetically we remark that, despite the fact that cavitation phenomena are now recognized to be initimately related to the population of "cavitation" nuclei in the incoming liquid stream, it is still too often the case that this distribution goes unmeasured. We must insist on this documentation for all cavitation experiments. Typical nuclei number distribution functions, $N(R_0)$ where R_0 is the nuclei radius in meters, are shown in figure 1; $N(R_0)$ is defined such that the number of nuclei with sizes between R_0 and $R_0 + dR_0$ is $N(R_0)dR_0$. We shall return a little later to discussion of the effects of the nuclei number distribution.

The present remarks will be confined to the cavitation noise produced by bubble cavitation in flows around bodies such as headforms or hydrofoils. Thus we shall be concerned with the behavior of cavitation bubbles in the presence of various flow phenomena such as pressure gradients, boundary layers, separation and turbulence. A great deal of research has been done on the dynamics and acoustics of cavitation bubbles in quiescent liquid (Knapp, Daily and Hammitt [1970]). It is known, for example, from both experiments and analysis that when a bubble in a quiescent liquid collapses close to a solid boundary a microjet forms on the bubble surface furthest from the solid boundary and reaches very high velocities (Plesset and Chapman [1970]). The current state of knowledge of this phenomena has recently been comprehensively reviewed by Blake and Gibson [1987]. Those authors reflect a current body of opinion in which these microjets are believed to be responsible for both the material damage and the noise created by cavitation.

Even for bubbles in a quiescent liquid, this view may need to be modified in the light of the recent observations by Kimoto [1987]. He simultaneously took high speed motion pictures and made local pressure measurements on the surface beneath a collapsing cavitation bubble in a quiescent liquid and observed the instantaneous loading on the surface, not only as a result of the microjet, but also as a result of the shock wave generated when the remnant cloud of bubbles collapses. It is significant

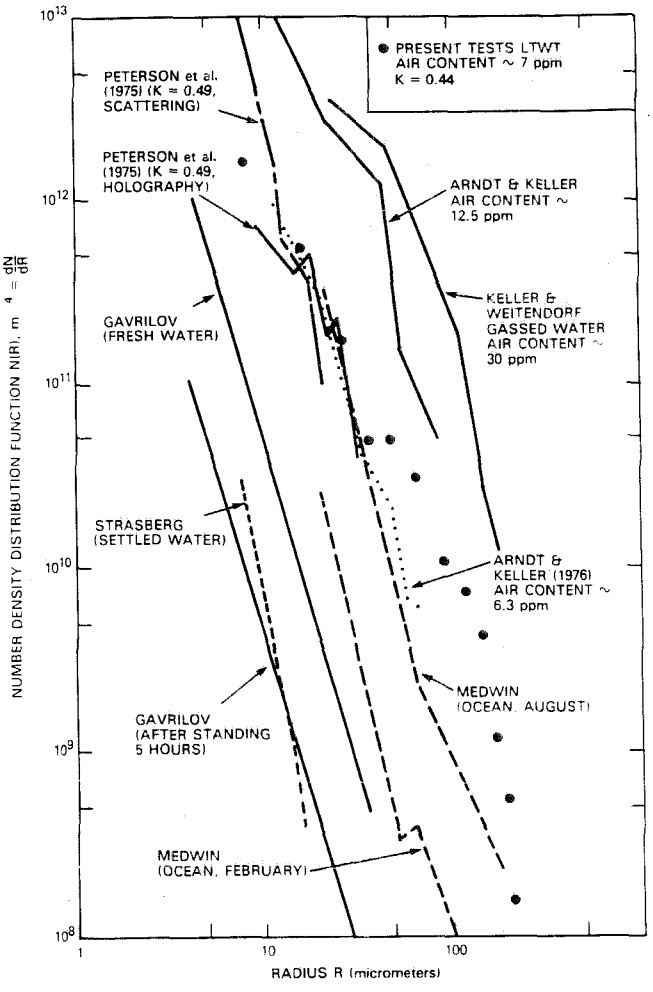

Figure 1. Typical nuclei number distribution functions. From Gates and Acosta [1978].

that the shock wave loading was usually a factor of two or three times larger than that due to the microjet. From the point of view of the acoustics, this means that the dominant acoustic pressure pulse may be generated by the remnant cloud collapse rather than by the microjet.

But one of the main issues which we would like to emphasize is that *none* of these observations have been made for cavitation around a headform or hydrofoil. Indeed, from the very earliest observations of Knapp and Hollander [1948] and Parkin [1952] down to the more recent observations (for example those of Blake, Wolpert and Geib [1977] or Kodama, Tamiya, Take and Kato [1979]), experimentalists have consistently commented on the distorted shapes which cavitation bubbles can take in flows around bodies. Indeed, all four of the above papers specifically mention the "hemispherical" shape which the traveling bubbles appear to assume. Why the bubbles take this shape and what effect these shapes have on the collapse process, resulting noise generation, and damage potential is largely unknown. The point here is that, although the macroscopic effects of boundary layers, separation and turbulence on cavitation have been known for some time (eg, Arakeri and Acosta [1973]), the effects of these flow phenomena on the dynamics of individual bubbles and therefore on the collapse mechanics and noise production for individual bubbles has only begun to be explored.

Several studies of the acoustic signals from single traveling cavitation bubbles have been carried out. In an early paper Harrison [1952] identified the first collapse as the time of noise generation. More recently Hamilton, Thompson and Billet [1982] (see also Hamilton [1981]) and Marboe, Billet and Thompson [1986] have initiated the kind of research which can lead eventually to a deeper understanding of the mechanics of cavitation noise. We have recently conducted some tests which complement the last two studies, and a description of some of the results will provide an illustration of the events and a framework in which to comment on future research directions.

2. OBSERVATIONS OF SINGLE BUBBLE DYNAMICS AND ACOUSTICS

A 5.59 cm. diameter ITTC headform (Hoyt [1966]) was fabricated from lucite. The hollow interior of this headform was filled with water and a ITC-1042 hydrophone placed in the water-filled interior (see figure 2). Because of the good acoustic impedance match between lucite and water, this arrangement allows the noise generated by the cavitation bubbles to reach the hydrophone relatively undistorted; reflected acoustic signals from other parts of the water tunnel only make their appearance after the important initial signal has been recorded.

This headform was installed in the low turbulence water tunnel (LTWT) at Caltech. In addition to the hydrophone, the headform was equipped with a novel device developed from instrumentation which had been used to measure volume fractions in multiphase flows. This device consisted of an axial sequence of 16 patch electrodes, 0.127 cm. long, 0.572 cm. wide and with a separation of 0.127 cm. These were located so as to cover the major extent of the cavitation region on the headform (see figure 2). (The electrodes were conveniently fabricated us-

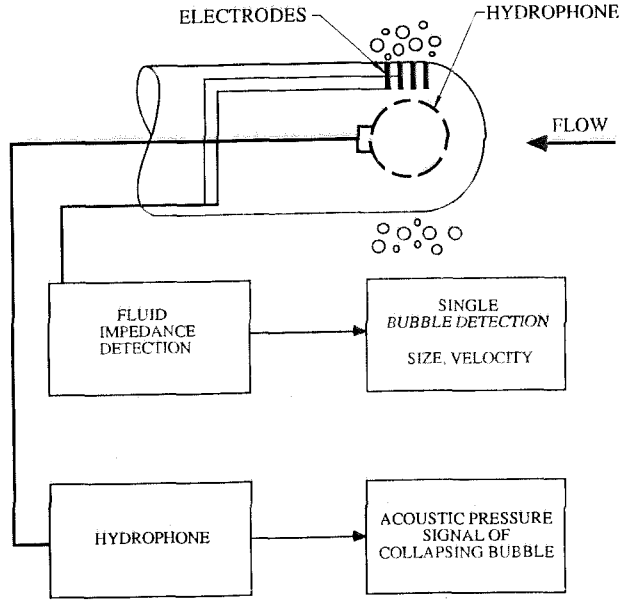

Figure 2. Schematic illustrating the instrumentation of the ITTC headform.

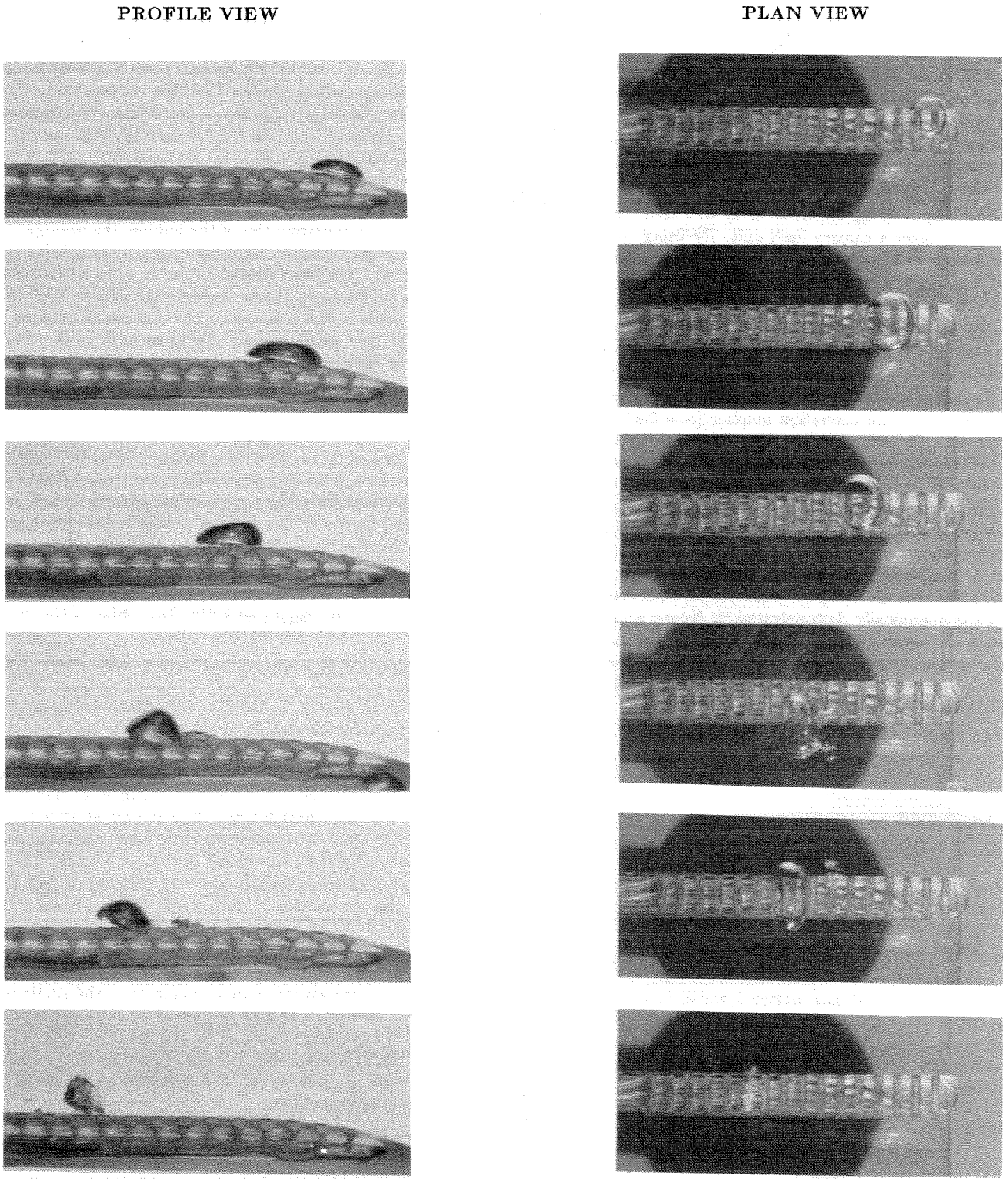

Figure 3. Photographs of cavitation bubbles during different stages of their life (flow is from right to left). Simultaneous plan and profile views are shown for a tunnel velocity of 8.4 m/s and a cavitation number, $\sigma = 0.47$. Total bubble lifetime is about 3ms and the six pairs of photographs represent roughly equal time increments within this lifetime. Scale is given by the electrode spacing which is 0.254 cm, center to center.

ing an electrically conducting epoxy which could be machined and polished together with the lucite.) A pattern of alternating electric potentials is applied to these electrodes and the electric current from each electrode is monitored. When a bubble passes over one of these electrodes the resistivity of the local conducting medium is changed, causing a change in the current from that electrode. This change is related to the position and volume of the bubble. Consequently, the electrode array allows passive detection and monitoring of individual cavitation bubbles.

The output of the electrode array was used, among other things, to trigger a camera flash unit. By using two cameras, simultaneous profile and plan photographs were taken of individual bubbles at a prescribed moment during their trajectory. Thus a whole series of bubbles could be inspected, all at the same point in their evolution. Furthermore, by simultaneously recording the acoustic signal from the hydrophone, one could correlate the noise with the geometry of these bubbles.

Examples of these photographs taken for a given tunnel speed (8.4 m/s) and cavitation number ($\sigma = 0.47$) are shown in figure 3. One of the first major observations is how similar and repeatable all the photographic observations are for a given trajectory position. The bubbles vary little in size or shape. They are far from being spherical and assume the slightly squashed "hemispherical" form sketched in figure 4, a shape which has been described by a number of other authors as mentioned previously. The volume/time history of the bubbles appears to follow the Rayleigh/Plesset equation in the manner originally demonstrated by Knapp and Hollander [1948] and Plesset [1949]. The uninitiated may wonder why all of the bubbles have close to the same size when the nuclei, as previously demonstrated, come in a wide range of sizes. We will address this phenomenon in the next section.

As the bubbles proceed through their growth phase, several features, sketched in figure 4, are consistently observed.

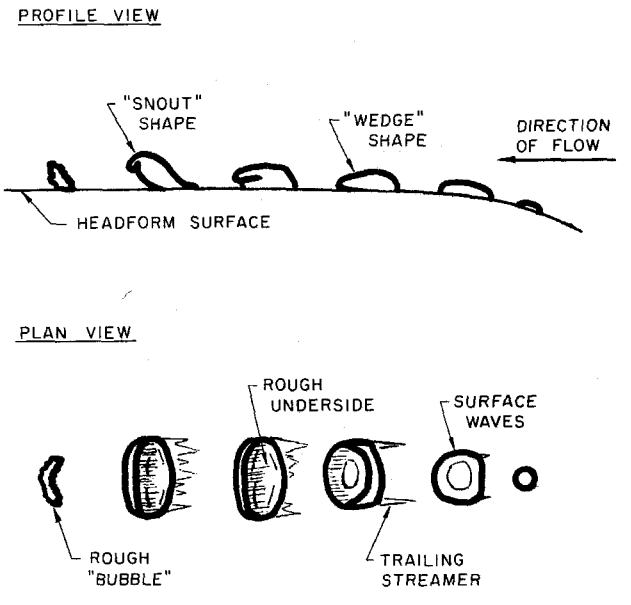

Figure 4. Schematic illustrating the various features of a cavitation bubble during different stages of its life.

As the bubbles approach their maximum size they become somewhat elongated in the direction normal to their motion while their thickness normal to the surface remains relatively constant. The ITTC headform possesses a laminar separation point just downstream of the tangent point of the surface contour. This separation appears to affect the bubble in several ways. First, the relatively flat undersurface of the bubble is seen to move away from the solid surface as it follows the separation streamline. Secondly, the undersurface appears to be effected by the disturbances caused by transition and turbulent reattachment since it becomes markedly roughened. Thirdly, at the two lateral extremities of the bubble, the passage of the bubble appears to cause highly localized attached cavitation producing the trailers sketched in figure 4 which look somewhat like tip vortices. These trailers may persist briefly after the main bubble has collapsed. The process of collapse also appears to have some common features such as the "snout" depicted in figure 4. It is clear that the bubble cloud which emerges from the first collapse is elongated in the direction perpendicular to the flow and also has a characteristic orientation in the profile view.

The process of a cavitation bubble's evolution will most likely vary from headform to headform and will depend on the state of the boundary layer, separation, and transition. It will also depend on the Weber number as well as the and Reynolds number. Furthermore, it seems clear that the acoustics (and damage potential) will depend upon the detailed mechanics of bubble collapse. Consequently, a deeper understanding of cavitation noise must depend on better knowledge of the detailed mechanics of bubble growth and collapse.

As virtually all previous investigators have discovered, we found that the noise is initiated during the moment of violent first collapse. Figure 5 presents two typical examples of the acoustic signal generated by a single bubble collapse. These signals are not filtered except for ultralow frequencies (D.C.). The hydrophone has a relatively flat response out to 80 kHz. In this sense our observations differ from those of Hamilton et al [1982] who high-pass filtered their signals at 10 kHz. The signals in figure 5 were obtained by a digital data aquisition system sampling the hydrophone output at 1 MHz. The general features of these signals are very consistent. An initial pressure rise accelerates to one or two positive peaks. These are presumably associated with the very large and positive volume accelerations which occur when the bubble volume passes through its minimum. The double peaks shown in the second example were somewhat more common than the single peaks of the first example and may be caused by the original bubble splitting in two before reaching its minimum volume. The remaining signal, while noisy, is quite repeatable and consists of a broad reduced pressure period followed by a gradual increase toward a broad maximum.

From these records and the photographs, data was obtained on the maximum bubble volume prior to the first collapse, the peak acoustic pressure and the impulse of the pressure peaks in the signals defined as

$$I = \int_{\substack{\text{long before} \\ \text{bubble collapse}}}^{\substack{\text{point where pressure} \\ \text{passes through zero}}} p \, dt \qquad (1)$$

or the area under the initial peak or peaks in the acoustic output. An example of the correlation between the maximum

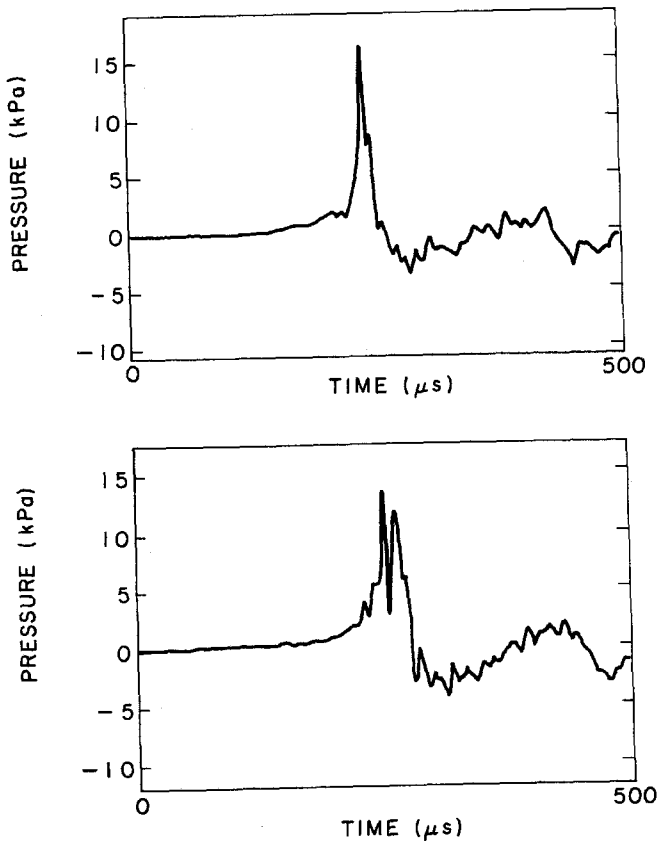

Figure 5. Typical acoustic pressure pulses generated by a single cavitation bubble collapse. Tunnel velocity = 9.1m/s, σ = 0.44.

volume and the acoustic impulse, I, is shown in figure 6.

This and other similar data have a number of interesting features. The data all appear to lie below an envelope which is close to a straight line passing through the origin. It seems that there is a maximum acoustic impulse which a collapsing bubble may generate from a certain maximum volume if it collapses in some particular but unknown way. It can, however, produce less than this maximum impulse if it collapses in other ways. The line plotted in figure 6 is a theoretical prediction discussed in the next section.

In closing, we comment that it would appear that there is still much to be learned from studies of individual cavitation bubbles in real viscous flows and that an improved understanding of these events is an esssential step in improving our understanding of cavitation noise.

3. SOME COMPARISONS WITH RAYLEIGH/PLESSET SOLUTIONS

In order to place the experimental results such as those of figure 6 in some analytic perspective, calculations were performed to evaluate how free stream nuclei of various sizes would respond to the pressure/time history they experience during flow around the ITTC headform. The known surface pressure distribution for that headform (eg. (Hoyt [1966]) was employed to construct the pressure/time history assuming no slip between the bubbles and the liquid and a certain offset

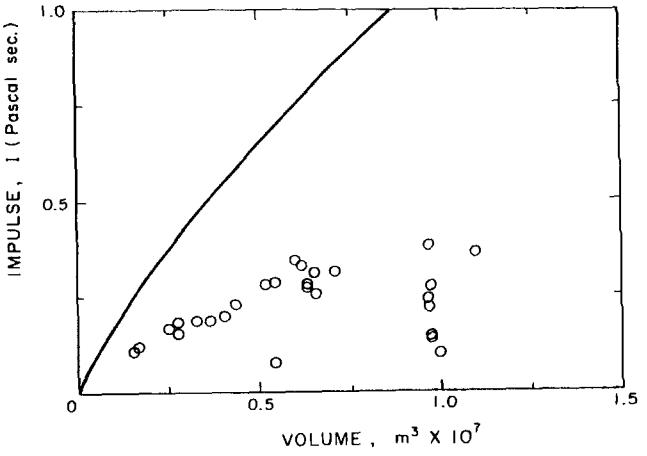

Figure 6. Experimental data showing the relationship between the acoustic impulse, I ($Pa \cdot s$), at the maximum bubble volume (m^3) for tunnel velocity of 9.1 m/s and $\sigma = 0.44$. Also shown by the solid line is an analytic result described in section 3.

from the stagnation streamline. Details will be provided in a later publication. The calculation was performed with various assumed equilibrium nuclei in the upstream flow, various free stream velocities, U, cavitation numbers and offsets from the stagnation streamline. The viscosity, density, ρ, and surface tension, S, of water at 20°C were employed in evaluating these effects in the Rayleigh/Plesset solution. For present purposes we will focus on the relationship between maximum volume and the magnitude of the acoustic pressure, p_A, which these calculations yield, that pressure being calculated as

$$p_A(r,t) = \frac{\rho}{4\pi r} \frac{d^2V}{dt^2} \tag{2}$$

when $V(t)$ is the volume of the bubble and r is the distance from the center of the bubble.

Figure 7 provides an example of the dependence of the maximum bubble radius on the original nuclei size for four different cavitation numbers. This figure illustrates several important phenomena which are too seldom mentioned even though they have been very clearly documented and discussed by Flynn [1964] in his excellent review. The first notable feature is that nuclei below a certain size (which depends upon the cavitation number) hardly grow at all and would therefore not contribute visible cavitation bubbles. This feature is quite accurately predicted by applying the static stability criterion of Johnson and Hsieh [1966] at each point along the bubble trajectory. The bubble is statically unstable if

$$\frac{R_L}{R_H} > \frac{8}{3} \frac{S}{\rho R_H U^2} \frac{1}{(-\sigma - C_{PMIN})} \tag{3}$$

where C_{PMIN} is the minimum pressure coefficient (-0.62 for the ITTC headform) and R_L is the local bubble size. The computations (and figure 7) show that so long as the bubble remains stable, then R_L is somewhere in the range $R_O < R_L < 2R_O$ for the common circumstances of interest here. Consequently, the critical nucleus size R_C is given by

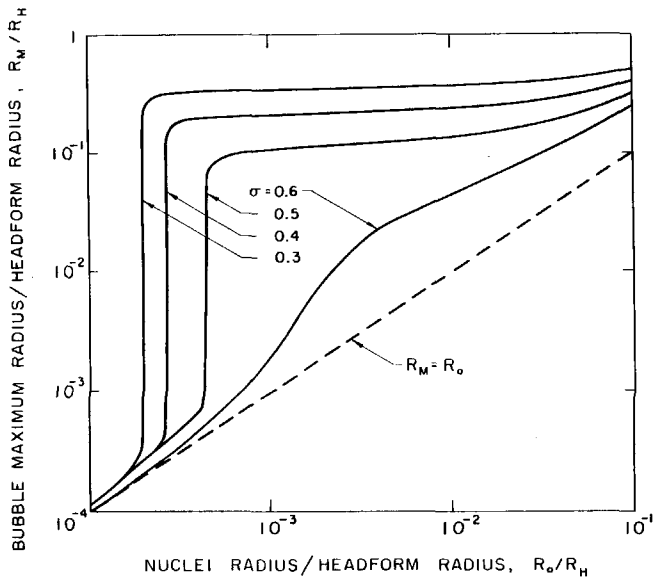

Figure 7. Maximum bubble radius, R_M, from Rayleigh/Plesset solution as a function of nuclei radius, R_0. Plotted for a Weber number, $S/\rho R_H U^2 = 0.000036$ (water with $R_M = 2.79$cm, $U = 9$ m/s) and various cavitation numbers, σ, as shown.

$$\frac{R_C \rho U^2}{S} \approx \frac{8\beta}{3(-\sigma - C_{PMIN})} \tag{4}$$

where β is approximately one-half. The results of this simple expression are presented in figure 8 along with data on the critical nuclei size obtained from the Rayleigh/Plesset solutions. The qualitative agreement is excellent and suggests a value of β slightly greater than 0.5. Note that the higher the velocity, U, the smaller the critical radius, R_C, and therefore the larger the number of nuclei involved in cavitation. As discussed later, this may have important consequences in the scaling of cavitation noise.

The other feature of figure 7 which is important to note is that virtually all nuclei greater than the critical size grow to ap-

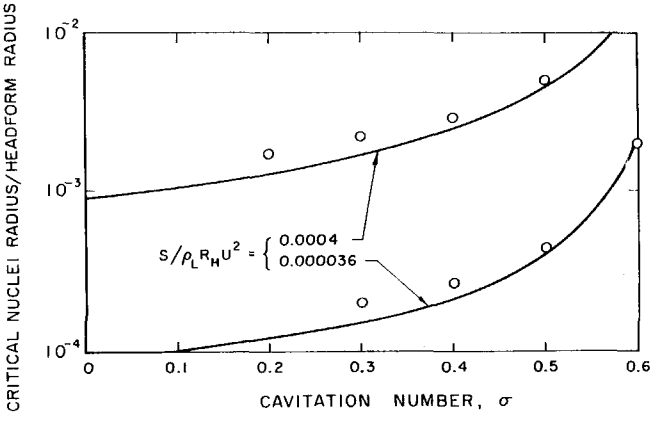

Figure 8. Points represent the critical nuclei radius/headform radius from Rayleigh/Plesset solutions for two different Weber numbers as indicated. The lines are the corresponding values using equation (4) with $\beta = 0.5$.

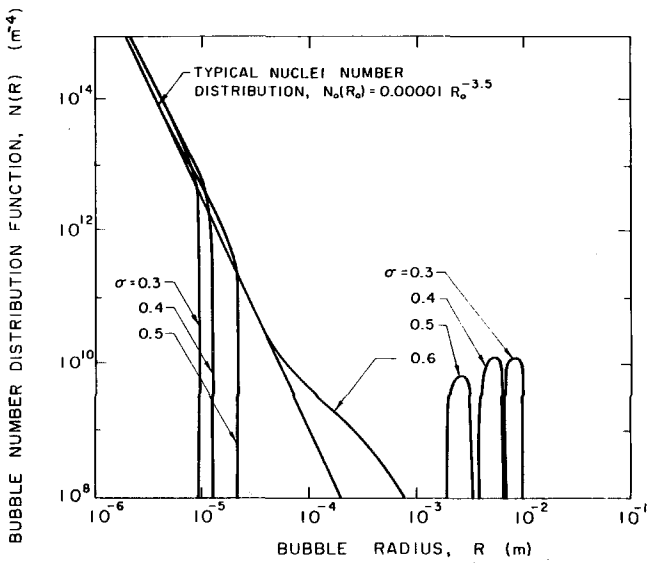

Figure 9. Number distribution functions, $N(R)$. Typical nuclei number distribution is represented by $N_0(R_0) = 0.00001 R_0^{-3.5}$ m^{-4}. Also shown are the resulting distributions for the maximum radius, $N_M(R_M)$, for the four different cases defined in figure 7.

proximately the same maximum size. The asymptotic growth rate of a cavitating nuclei is a function only of the pressure and not of the initial nuclei size. Since the time available for growth is also independent of the nuclei size, it follows that the maximum size obtained will be quite uniform for all cavitating nuclei. This explains why the bubbles observed in most traveling bubble cavitation flows are all of similar size even though they originate from nuclei of quite different size.

This phenomenon can be illustrated in a different way by constructing from figure 7 and a nuclei number distribution function, $N_O(R_O)$, the number distribution function for the observed cavitation bubbles at their point of maximum growth. Such a distribution is presented in figure 9 using

$$N_O(R_O) = N^*/R_O^n \tag{5}$$

where R_0 is in m, N_0 is in m^{-4}, $N^* = 0.00001$ and $n = 3$ or 4 would be typical of the distributions in the center of figure 1. Using this relationship the number distributions for the bubble maximum size are presented in figure 9. Note the well defined peaks which constitute the number distribution in the spectrum of visible cavitation bubbles.

We now turn to the noise produced by individual bubbles. First note that the subcritical nuclei which essentially behave quasistatically yield volume histories, $V(t)$, which, according to the relation (2), would not produce any measurable noise. Only supercritical nuclei, which exhibit the kind of castrophic collapse characteristic of cavitation, will contribute to the noise. This is a feature of the cavitation noise problem which is not widely recognized. Furthermore, the critical size, and consequently the supercritical nuclei population, will depend, not only on the cavitation number, but also on the Weber number, $\rho U^2 R_H/S$.

The magnitude of the noise predicted by the Rayleigh/Plesset calculations will be examined while recognizing, of

course, that these calculations may be of limited applicability during the collapse phase when the bubble typically departs from a spherical shape. For reasons to be discussed in a later paper, we choose to compare the experimental measurements with the acoustic impulse from the first collapse in the Rayleigh/Plesset calculation where this is defined as the integral over the entire positive peak in the acoustic pressure. The non-dimensional impulse, I^*, is defined as

$$I^* = 4\pi I/\rho R_H U \tag{6}$$

where we choose to evaluate the noise at a radius, r, from the bubble equal to the headform radius, R_H, since this is the location of the hydrophone in the experiment discussed in the last section. This impulse I^* is plotted in figure 10 against the maximum volume of the bubbles non-dimensionalized by R_H^3. A number of investigations (for example, Fitzpatrick and Strasberg [1956] and Hamilton, Thompson and Billet [1982]) have suggested that the magnitude of the acoustic signal should be related to the maximum size of the bubble, and this is born out in figure 10 where the data for a range of cavitation numbers and two Weber numbers are contained within a fairly narrow envelope. The median line is converted to dimensional values and is plotted in figure 6 where it is compared with the experimental data. It is quite striking that the envelope of the maximum impulses from the experiments is within a factor of two of the impulse predicted by the Rayleigh/Plesset equation. This suggests that, despite the departure from spherical shape during collapse, the Rayleigh/Plesset solutions come close to predicting the magnitude of the noise generated by individual bubbles and, consequently, that the noise magnitude is related to volume and not to shape.

As widely discussed by many authors, the duration of the impulse (as opposed to its magnitude) is much better understood. Here the duration, T^*, is defined as the time between the points for which $d^2V/dt^2 = 0$ prior to and after the first collapse. This time, T^* is simply related to the total collapse

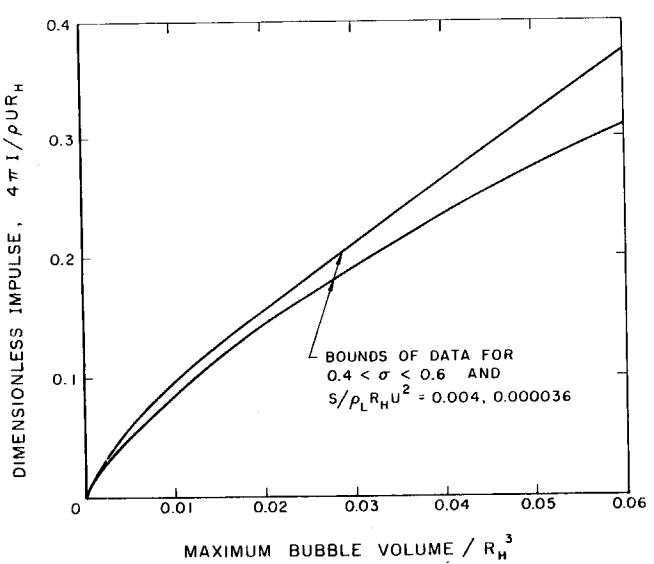

Figure 10. The relationship between the dimensionless acoustic impulse, $4\pi I/\rho U R_H$, and the maximum bubble volume prior to collapse. Data for $0.4 < \sigma < 0.6$ and $S/\rho_L R_H U^2 = 0.004$ and 0.000036 lie within the envelope shown.

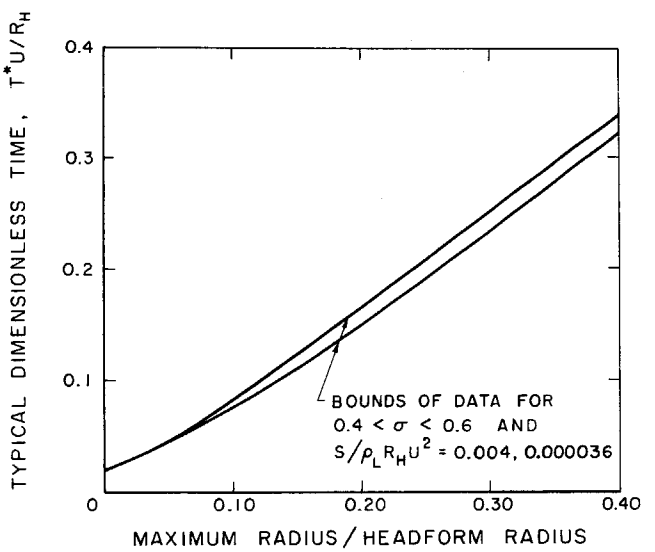

Figure 11. Relationship between the duration of the acoustic impulse, T^*, and the maximum bubble radius prior to collapse. Data for $0.4 < \sigma < 0.6$ and $S/\rho_L R_H U^2 = 0.004$ and 0.000036 lie within the envelope shown.

time used by many authors (e.g., Blake et al [1977], Arakeri and Shanmuganathan [1985]). Like the collapse time, it will be given approximately by

$$T^* = k\frac{R_M}{U}\left(\frac{2}{\sigma}\right)^{\frac{1}{2}} \tag{7}$$

where k is some constant of order unity. It follows that the dimensionless impulse duration T^*U/R_H should be close to being a function only of R_M/R_H and this is confirmed by the Rayleigh/Plesset solutions, the results for which are shown in figure 11. Note that the results lie within a narrow envelope and that the slope of the narrow envelope is close to unity. The frequency spectra for cavitation noise will be closely related to the period, T^*, and the many higher harmonics which result from the highly nonlinear nature of the signal within this period. In conclusion, since both the magnitude and frequency content of individual bubble noise seem to be fairly well predicted, it would seem that one might be optimistic about predictions for the magnitude and spectral content of a flow containing many bubbles.

Scaling of cavitation noise with velocity and cavitation number is a subject of continuing concern in interpreting water tunnel model tests. The scaling with velocity, U, is particularly poorly understood. Correlation of experimental data on the acoustic pressure with U^n yields values of $n \approx 2$; for example the $n = 2.2$ data of Lush [1975] for a cavitating venturi and values between $n = 1.5$ and 2 from the experiments of Blake et al [1977] and Hamilton et al [1982]. Like the analytical models discussed in those references, the present theory would, at first glance, yield an $n = 2$ dependence because the impulse and the frequency of collapses both vary linearly with U if the nuclei number distribution and the critical nuclei radius remain the same for all velocities. However, as the results of Hamilton et al [1982] graphically illustrate, these conditions are rarely met. They found that the number of collapses per second increased with velocity at a rate much higher than linearly. Probably

this was due to smaller nuclei becoming activated. But it is also true that the nuclei number distribution in the working section of a water tunnel may vary significantly with velocity even when the nuclei number distribution in the rest of the tunnel remains unchanged. It is therefore difficult to interpret the existing data without more careful documentation of the nuclei number distributions existing at each operating point.

4. BUBBLE INTERACTIONS

We now turn to a discussion of the circumstances under which there is significant interaction between bubbles and the nature of those interactions. In the idealized and relatively small scale environment of a water tunnel one can produce flows in which single, non-overlapping cavitation events occur. However, in practice, cavitation events usually overlap and may therefore interact. This is particularly true when the scale of the flow is increased while the nuclei number density remains the same. Then the cavitation region contains more bubbles and the chances of significant interaction occur. Since most model to prototype scaling involves such an extrapolation, it is important to consider the possibility of interaction in the prototype even though it may be insignificant on the model scale.

While the dynamics of bubbly flows have been extensively studied for many years (see, for example, van Wijngaarden [1968, 1972]), it was not until quite recently that the possible relevance to cavitating flows of the interactive effects implicit in those two-phase flow models has been considered. A number of experimental observations motivated such investigations. As early as 1969, Erdmann, et al [1969] noticed an unexplained sharp decrease in the level of traveling cavitation bubble noise on hydrofoils when the cavitation became extensive, and this same observation has subsequently been made by many investigators. During their observations of traveling bubble cavitation on a Schiebe headform, Marboe, et al [1986] found that the noise spectra tended to shift toward lower frequencies than those expected from single bubble dynamics. They suggested that this shift might be due to asymmetric bubble collapse, though the lower frequencies associated with clouds of bubbles (see below) could also provide a possible explanation. Somewhat similar results have also been presented by Arakeri and Shanmuganathan [1985] who observed that when they seeded

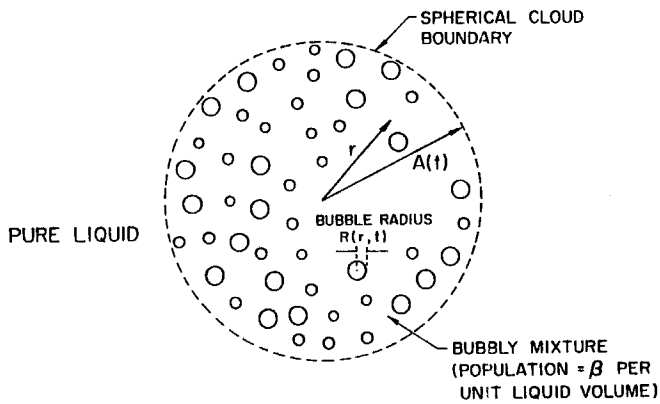

Figure 12. Schematic of a spherical cloud of bubbles.

a cavitating flow so that it contained a greater nuclei number density, the maximum size to which those nuclei grew was decreased, a fact which clearly indicates interaction between the bubbles.

Another type of collective effect occurs because many cavitating flows seem to be susceptible to a relatively low frequency instability so that cavitation takes the form of a periodic growth and collapse of a cloud or group of bubbles. In particular, Mørch [1980, 1981, 1982] and Hanson, Kedrinskii and Mørch [1982] correlated the collapse of clusters of cavitation bubbles with the creation of strong shock waves. Other examples of the formation and collapse of clouds of cavitation bubbles are contained in Brennen, et al [1980] and Bark [1986]. Often the clouds occur in the core of a shed vortex which adds greatly to the complexity of the vortex dynamics and of the bubble dynamics.

One of the first attempts to analyze bubble interaction effects was made by van Wijngaarden [1964] who considered the case of a uniform layer of bubbles next to a solid wall. Like virtually all of the other analyses which followed, van Wijngaarden simultaneously solved space-averaged continuity and momentum equations of the form

$$(1+\beta\tau)\,\nabla\cdot\underline{u} = \frac{D(\beta\tau)}{Dt} \tag{8}$$

$$(1+\beta\tau)\,\nabla p = -\rho\frac{D\underline{u}}{Dt} \tag{9}$$

where $u(\underline{x},t)$ and $p(\underline{x},t)$ are the fluid velocity and pressure fields, $\tau(\underline{x},t)$ is the bubble volume, ρ is the liquid density and $\beta(\underline{x},t)$ is the population of bubbles per unit liquid volume. These equations neglect relative motion between the bubbles and the liquid which has subsequently been shown to have a negligible effect in the acoustics of the mixture (d'Agostino and Brennen [1989]). Furthermore, the effects of liquid compressibility have been omitted (for their inclusion see d'Agostino and Brennen [1989]) as have the viscous effects in the equation of motion (9). The fundamental bubble interaction effect is evaluated by solving equations (8) and (9) simultaneously with the Rayleigh/Plesset equation relating the location bubble volume, τ, to the "local" pressure, $p(\underline{x},t)$. It is normally assumed that the void fraction, $\alpha = \beta\tau/(1+\beta\tau)$ is sufficiently small so that one can define a local pressure which, to an individual bubble, appears to be the pressure at infinity. However, Chahine [1982a,b] has considered higher order interactions in which a bubble is effected by the local pressure perturbation fields surrounding its neighbors.

This system of equations contains important nonlinear terms which seem to preclude analytic solution. Consequently, most of the analyses focus on solutions to the linearized forms of these equations. Even then, solutions have only been explored for geometrically simple flows and geometrics. Perhaps the simplest of these is the spherical cloud of bubbles of mean radius A_0, mean void fraction α_0, containing bubbles of mean radius R_0 and surrounded by pure liquid (see figure 12). As shown by d'Agostino and Brennen [1983, 1988] (see also Omta [1987]), this spherical cloud has its own series of natural frequencies, ω_n, corresponding to different natural modes, n, and given by

$$(i)\quad \omega_\infty = \omega_B$$

$$(ii)\quad \omega_n = \omega_B \left[1 + \frac{4}{3\pi^2}\,\frac{A_0^2\alpha_0}{R_0^2}\,\frac{1}{(2n-1)^2}\right]^{-\frac{1}{2}} ;\, n = 1, 2, \ldots \tag{10}$$

where ω_B is the natural frequency of an individual bubble in an infinite liquid (Plesset and Prosperetti [1977]). The above represents an infinite number of frequencies, the lowest of which is given by

$$\omega_1 = \omega_B \left[1 + \frac{4}{3\pi^2}\,\frac{A_0^2\alpha_0}{R_0^2}\right]^{-\frac{1}{2}} \tag{11}$$

All the natural frequencies are contained within the interval $\omega_1 < \omega_n < \omega_B$ with increasingly close packing near ω_B as n becomes large. Furthermore, it is clear that the size of this interval is determined by the parameter $A_0^2\alpha_0/R_0^2$. For large values of this parameter, the cloud natural frequencies can be much smaller than ω_B. Thus $A_0^2\alpha_0/R_0^2$ determines the degree of significant bubble interaction. Note that even when α is very small, there may still be significant interactions if the cloud is much larger than the individual bubbles.

The response of a spherical cloud to forced oscillations was also examined. At frequencies $0 < \omega < \omega_B$ the response consists of the expected resonances at each of the natural frequencies and with amplitudes of oscillation which do not vary greatly with radial location. However, when the cloud is subjected to frequencies above ω_B, quite a different kind of response is encountered. This consists of significant amplitudes occurring only in a surface layer of the cloud; the interior is essentially shielded by this surface layer. This shielding effect may have important consequences for acoustics of cavitating hydrofoils or propellers. Characteristic bubble dynamic damping was also included in the analysis (d'Agostino and Brennen [1989]), and a typical result is shown in figure 13 where the response in terms of amplitude of bubble radius oscillation at the surface of the cloud is presented with and without damping.

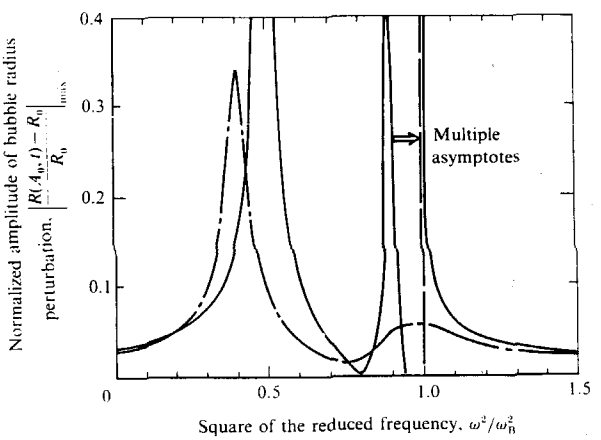

Figure 13. A typical non-dimensional amplitude of bubble oscillation at the surface of a spherical cloud showing the difference between the response in the absence of damping (solid line) and the response when typical damping is included (dot-dash line) (see d'Agostino and Brennen [1989]).

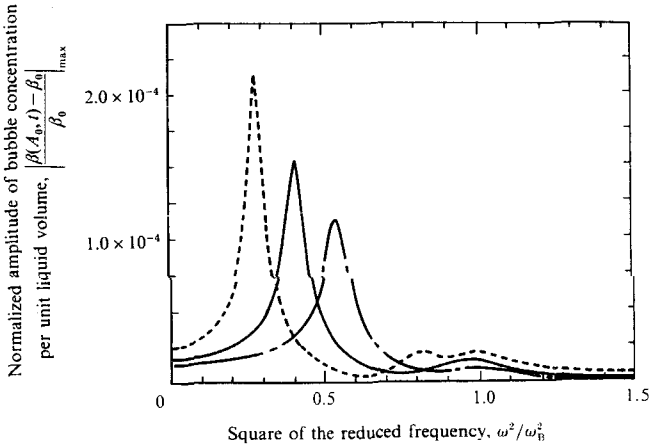

Figure 14. Typical damped responses of a spherical cloud of bubbles for various values of $3\alpha_0(1-\alpha_0)A_0^2/R_0^2$ of $\pi^2/4$(solid line), $\pi^2/8$ (dot-dash line) and $\pi^2/2$ (dotted line) (from d'Agostino and Brennen [1989]).

It is important to note that the higher frequencies, including the bubble natural frequency, are much more attenuated than the first cloud natural frequency. Consequently, if the parameter $\alpha_0 A_0^2/R_0^2$ is greater than unity, one should expect to see a dominant response, not at the bubble natural frequency, but at the cloud natural frequency. Three such damped responses for different $\alpha_0(1-\alpha_0)A_0^2/R_0^2$ are shown in figure 14.

In this first example there was clearly no steady component of the flow, and therefore we sought another simple example of a flow in which the interactions between cavitating bubbles could be examined. A suitable characteristic flow in which the bubble size linearization is still tenable is the planar flow over a wavy surface of small amplitude (see figure 15). The solution to this problem was presented in d'Agostino, Brennen and Acosta [1988]. It transpires that the crucial parameter is similar to that for the spherical cloud; in this case we define a special Mach number, M as

$$M^2 = \frac{4\pi\beta U_0^2 R_0}{\omega_B^2 - k^2 U_0^2} \tag{12}$$

where U_0 is the free stream velocity and k is the wave number of the wavy wall. This corresponds to a Mach number based on U_0 and the sonic speed of the bubbly mixture at the frequency kU_0. Consider first the case of a fixed wall geometry (with a single wavenumber, k) and vary the free stream velocity, U_0. It then transpires that there are *three* separate regimes of flow rather than the *two* which occur in single phase flow (subsonic and supersonic). At the lowest speeds ($kU_0 < \omega_B$, $M < 1$) the flow is "subsonic," the equations are elliptic and the behavior is similar to that for single-phase subsonic gas flow. In an intermediate range of speeds ($kU_0 < \omega_B$, $M > 1$), the flow is "supersonic," the equations are hyperbolic and the flow is similar to that for single-phase, supersonic gas flow. However, in bubbly cavitation flow there is an additional, higher speed regime of flow which we have termed "super-resonant" ($kU_0 > \omega_B$, $M^2 < 0$) which has no single phase analogy and in which the equations again become elliptic.

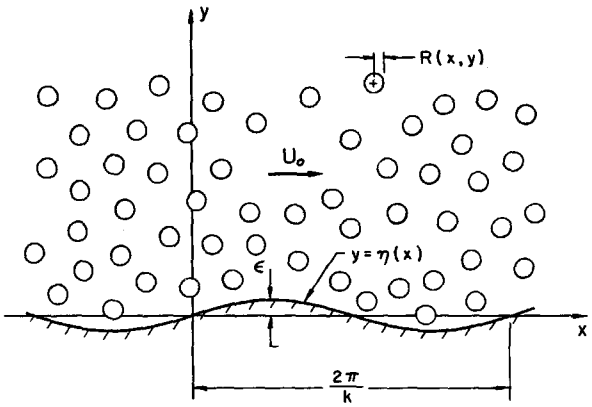

Figure 15. Schematic of a bubbly liquid flow over a wave-shaped surface.

The same fundamental solution was also used (d'Agostino, Brennen and Acosta [1988]) to analyze the bubbly cavitation flow at a speed, U_0 over a Gaussian-shaped wall projection or bump containing a spectrum of wave numbers, k. The results can be written in terms of integrals over the wave number. In the absence of bubble dynamic damping these integrals are necessarily singular at the two critical points, $M = 1$ and $kU_0 = \omega_B$, and hence the inclusion of appropriate damping is important. Some typical bubble amplitude responses to a Gaussian-shaped bump of typical width, a, are shown in figure 16 as a function of a coordinate x in the mean direction of flow. The three cases presented correspond to three different reduced velocities, $U_0/a\omega_B$, but are for a given $\omega_B a/c_M$ where c_M, is the mean sonic speed for the bubbly mixture. Note that for the low value of the reduced speed the response is essentially quasistatic and symmetric with respect to $x = 0$, the line of symmetry of the bump. However, as U_0 is increased the response of the bubbles is delayed and hence the largest bubble radii occur some distance beyone the maximum projection.

The pressure in the flow is perturbed in a manner very similar to the bubble volume. It is of interest to examine these pressure perturbations since they yield clues as to how the bubbles and the liquid pressure may effect one another in other cavitating flows. The pressure perturbations at the solid surface for the typical cases used for figure 16, are presented in figure 17. For the smallest reduced velocity,the pressure distribution is much as one would expect for incompresible potential flow. Note, however, that since the bubble dynamics become more important as the reduced velocity increases the pressure becomes much less symmetric. The bubble growth tends to relieve or increase the pressure in the cavitation zone downstream of the maximum projection. Finally we note that these solutions exhibit the phenomenon that increasing the number of nuclei decreases the amplitude of bubble growth, an effect which, it has been previously noted, was observed experimentally by Arakeri and Shanmuganathan [1985].

The preceding discussion has concerned linear solutions to the interaction problem. On the other hand, cavitation noise is generated during a highly nonlinear process. The role played by interactions in the dynamics of the collapse process are much harder to evaluate analytically, though a number of

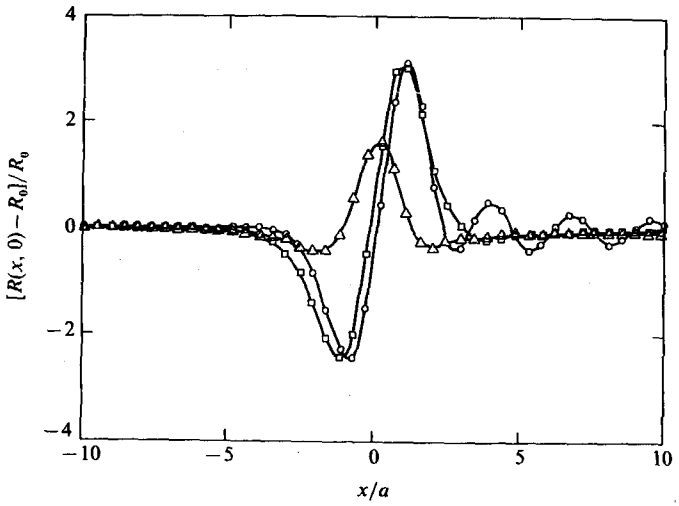

Figure 16. Bubble amplitude response for a bubbly flow over a Gaussian-shaped bump of typical width a centered at $x = 0$ as a function of position. Results are shown for three different reduced velocities given by $(U_0\pi/a\omega_B)^2 = 0.5(\Delta), 1(\square)$ and $2(0)$.

efforts have been made. Chahine [1982a,b] has constructed a model for a cloud of cavitating bubbles collapsing near a wall and concludes that the collective effect will be to increase the violence of the collapse. Omta [1987] has extended the linear analysis for a spherical cloud to include some nonlinear effects. At the other extreme,Mørch [1980,1981] and Hanson et al [1982] speculate that the nonlinear effects result in the formation of a shock wave, the progress of which constitutes the collapse of a cloud of bubbles. It is clear that more experimental and analytical work is necessary to clarify our understanding of these nonlinear interactions.

5. CONCLUSIONS

In this paper we have tried to highlight aspects of our cur-

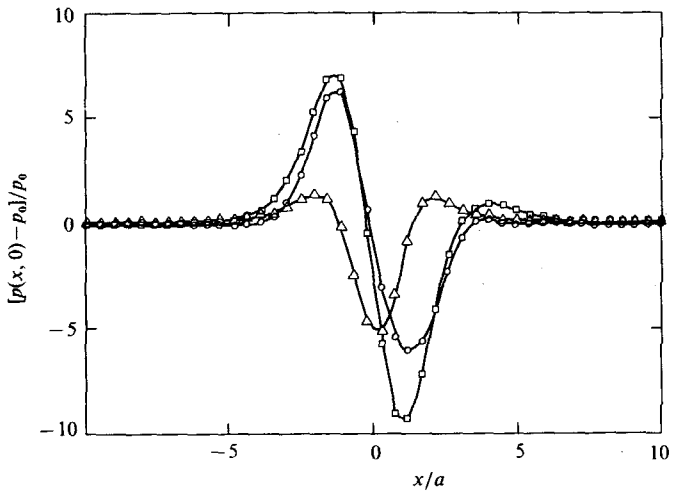

Figure 17. The perturbation in the pressure at the surface for the same solutions as presented in figure 16.

rent knowledge of cavitation and cavitation noise which would benefit from further research.

First, it is clear that cavitation experiments need to be fully documented through monitoring of the nuclei number distribution functions. It is also important to recognize that the relevant distribution is that in the working section and that this distribution may not only vary with time but with the tunnel operating point. We argue that it is important to integrate the measured distributions into analytical methods for the prediction of cavitation such as the Rayleigh/Plesset solutions presented here.

Secondly, we have tried to illustrate by example that much remains to be learned about how individual traveling cavitation bubbles are affected by viscous flow phenomena such as boundary layer separation and transition. In the experimental observations described, the bubble behaves quite differently from bubbles in quiescent liquid. It seems self-evident that a deeper understanding of cavitation damage and noise in flows around bodies will depend on better documentation of the in situ bubble dynamics.

We presented several numerical solutions of the Rayleigh/ Plesset equation to demonstrate that the predicted acoustic impulse generated during collapse comes to within about a factor of two of the observed impulses measured from experimentally from individual bubbles. Since the durations of the impulse also agree quite well, one may be optimistic that both the magnitude and spectra of cavitation noise may be predicted in the near future provided the nuclei number distribution problems are thoroughly confronted.

Finally, we have presented a summary of the bubble interaction problems and phenomena. The collective dynamics within a cloud of bubbles can be quite different from that of its individual constituent bubbles if a parameter like $\alpha A^2/R^2$ is of order one or larger, where α is the void fraction, A is the typical cloud dimension and R the individual bubble radius. Most of the analyses to date are linearized solutions of the problems. In order to properly identify those circumstances under which bubble interactions are important, it is necessary to continue the exploration of these phenomena both experimentally and theoretically. Often, for example, cavitating flows consist, not of a cloud of bubbles, but of a thin layer of bubbles next to a surface, yet there exists no analytical treatment of such a distribution.

6. ACKNOWLEDGMENTS

The authors are very grateful for the support of the Office of Naval Research. The preparation of this paper and the research program at Caltech is supported by ONR under Contract N00014-85-K-0397. We should also like to thank D. Hart and S. Kumar for their continuing help.

REFERENCES

Arakeri, V.H. and Acosta, A.J. 1973. Viscous Effects in the Inception of Cavitation on Axisymmetic Bodies, *ASME Journal of Fluids Engineering*, Vol. 95, pp. 519-527.

Arakeri, V.H. and Shanmuganathan, V. 1985. On the Evidence for the Effect of Bubble Interference on Cavitation Noise, *Journal of Fluid Mechanics*, Vol. 159, pp. 131-150.

Arndt, R.E.A. and Keller, A.P. 1976. Free Gas Content Effects on Cavitation Inception and Noise in a Free Shear Flow. *IAHR Symposium Two Phase Flow Cavitation Power Gener. Syst.*, Grenoble, France, pp. 3-16.

Bark, G. 1986. Development of Violent Collapses in Propeller Cavitation. *ASME International Symposium on Cavitation and Multiphase Flow Noise*, FED-Vol. 45, pp. 65-76.

Blake, J.R. and Gibson, D.C. 1987. Cavitation Bubbles Near Boundaries. *Ann. Rev. Fluid Mechanics*, Vol. 19, pp. 99-123.

Blake, W.K., Wolpert, M.J. and Geib, F.E. 1977. Cavitation Noise and Inception as Influenced by Boundary Layer Development on a Hydrofoil. *Journal of Fluid Mechanics*, Vol. 80, pp. 617-640.

Blake, W.K. 1986. Mechanics of Flow-Induced Sound and Vibration, Volume 1, Chapter 6, *Introduction to Bubble Dynamics and Cavitation.* Academic Press, pp. 370-425.

Brennen, C.E., Oey, K. and Babcock, C.D. 1980. On the Leading Edge Flutter of Cavitating Hydrofoils. *J. Ship. Research*, Vol. 24 (3), pp. 135-146.

Chahine, G.L. 1982a. Pressures Generated by a Bubble Cloud Collapse. *ASME Cavitation and Polyphase Flow Forum*, 1982, pp. 27-30.

Chahine, G.L. 1982b. Cloud Cavitation Theory. *14th Symposium on Naval Hudrodynamics*, August 1982, Session I, p. 51.

d'Agostino, L. and Brennen, C.E. 1983. On the Acoustical Dynamics of Bubble Clouds. *ASME Cavitation and Multiphase Flow Forum*, Houston, TX, June 1983.

d'Agostino, L., Brennen, C.E. and Acosta, A.J. 1988. Linearized Dynamics of Two-Dimensional Bubbles and Cavitating Flows Over Slender Surfaces. *Journal of Fluid Mechanics*, Vol. 192, pp. 485-509.

d'Agostino, L. and Brennen, C.E. 1988. Acoustical Absorption and Scattering Cross-sections of Spherical Bubble Clouds. *J. Acoust. Soc. of Amer.*, Vol. 84 (6), pp. 2126-2134.

d'Agostino, L. and Brennen, C.E. 1989. LInearized Dynamics of Spherical Bubble Clouds. *Journal Fluid Mechanics.*, Vol. 199, pp. 155-176.

Erdmann, H., Hermann, D., Norsback, M., Quinkert, R. and Sudholf, H. 1969. Investigation of the Production of Noise by the Propeller Particularly with Regard to the Combined Acoustic Problem – Work Segments II and III. Battelle Institute E.V. Frankfurt Am Main, 30 April 1969.

Fitzpatrick, H.M. and Strasberg, M. 1956. Hydrodynamic Sources of Sound. *First Symposium on Naval Hydrodynamics*, Washington, D.C., pp. 241-280.

Flynn, H.G. 1964. Physics of Acoustic Cavitation in Liquids. In *Physical Acoustics*, Volume - Part B, editor W.P. Mason, Academic Press.

Gates, E.M. and Acosta, A.J. 1978. Some Effects of Several Free-Stream Factors on Cavitation Inception on Axisymmetric Bodies. *12th Symposium Naval Hydrodynamics*, Washington, D.C.

Gavrilov, L.R. 1970. Free Gas Content of a Liquid and Acousti-

cal Technique for its Measurements. *Sov. Phys. - Acoust.* (Engl. Transl.), Vol. 15, pp. 285-295.

Hamilton, M.F. 1981. Travelling Bubble Cavitation and Resulting Noise. Appl. Res. Lab., Penn. State, Tech. Mem. TM 81-76.

Hamilton, M.F., Thompson, D.E. and Billet, M.L. 1982. An Experimental Study of Traveling Bubble Cavitation Noise. *ASME International Symposium on Cavitation Noise*, pp. 25-33.

Hanson, I., Kedrinskii, V. and Mørch, K.A. 1982. On the Dynamics of Cavity Clusters. *J. Phys. D: Appl. Phys.*, Vol. 15, pp. 1725-1734.

Harrison, M.F. 1952. An Experimental Study of Single Bubble Cavitation Noise. *Jour. Acoust. Soc. of Am.*, Vol. 24, No. 6, pp. 776-782.

Hoyt, J.W. 1966. Wall Effect on I.T.T.C. Standard Head Shape Pressure Distribution. Contribution to 11th International Towing Tank Conference.

Johnson, V.E. Jr. and Hsieh, T. 1966. The Influence of Gas Nuclei on Cavitatin Inception. *Proc. Sixth Symposium on Naval Hydrodynamics*, Washington, D.C.

Keller, A.P. and Weitendorf, E.A. 1976. Influence of Undissolved Air Content on Cavitation Phenomena at the Propeller Blade and on Induced Hull Pressure Amplitudes. *IAHR Symp. Two Phase Flow Cavitation Power Gener. Syst.*, Grenoble, France, pp. 65-76.

Kimoto, H. 1987. An Experimental Evaluation of the Effects of a Water Mircojet and a Shock Wave by a Local Pressure Sensor. *International Symposium on Cavitation Research Facilities and Techniques*, ASME FED Vol. 57, pp. 217-224.

Knapp, R.T. and Hollander, A. 1948. Laboratory Investigations of the Mechanism of Cavitation. *Trans. ASME*, July 1948, p. 419.

Knapp, R.T., Daily, J.W. and Hammitt, F.G. 1970. *Cavitation.* McGraw-Hill.

Kodama, Y., Tamiya, S., Take, N. and Kato, H. 1979. The Effect of Nuclei on the Inception of Bubble and Sheet Cavitation on Axisymmetric Bodies. *Proc. ASME International Symposium on Cavitation Inception* (ed. W. B. Morgan), pp. 75-86.

Lush, P.A. 1975. Noise from Cavitation in Venturi-type Sections. *Proc. Fifth Conference on Fluid Machinery*, Vol. 1, Akademiai Kiado, Budapest, pp. 627-638.

Marboe, R.C., Billet, M.L. and Thompson, D.E. 1986. Some Aspects of Traveling Bubble Cavitation and Noise. *ASME International Symposium on Cavitation and Multiphase Flow Noise*, FED Vol. 45, pp. 119-126.

Medwin, H. 1970. In Situ Acoustic Measurement of Bubble Populations in coastal Ocean Waters. *J. Geophysic. Res.*, Vol. 75, pp. 599-611.

Medwin, H. 1977. In Situ Acoustic Measurements of Microbubbles at Sea. *J. Geophysic. Res.*, Vol. 82, pp. 921-976.

Mørch, K.A. 1980. On the Collapse of Cavity Cluster in Flow Cavitation. *Proceedings of the 1st International Conference on Cavitation and Inhomogeneities in Underwater Acoustics.* Springer Series in Electrophysics (Springer, New York), Vol. 4, pp. 95-100.

Mørch, K.A. 1981. Cavity Cluster Dynamics and Cavitation Erosion. *ASME Cavitation and Polyphase Flow Forum*, pp. 1-10.

Mørch, K.A. 1982. Energy considerations on the collapse of cavity cluster. *Appl. Sci. Res.* Vol. 38, p. 313.

Omta, R. 1987. Oscillations of a Cloud of Bubbles of Small and Not So Small Amplitude. *J. Acoust. Soc. Am.*, Vol. 82, pp. 1018-1033.

Parkin, B.R. 1952. Scale Effects in Cavitating Flow. Ph.D. Thesis, California Institute of Technology.

Peterson, F.B., Danel, F., Keller, A.P. and Lecoffre, Y. 1975. Determination of Bubble and Particulate Spectra and Number Density in a Water Tunnel with Three Optical Techniques. *Proc. 14th ITTC*, Ottawa, Vol. 2, pp. 27-52.

Plesset, M.S. 1949. The Dynamics of Cavitation Bubbles. *ASME Journal of Applied Mechanics*, Vol. 16, pp. 228-231.

Plesset, M.S. and Prosperetti, A. 1977. Bubble Dynamics and Cavitation. *Ann. Rev. Fluid Mech.*, Vol. 9, pp. 145-185.

Plessset, M.S. and Chapman, R.B. 1970. Collapse of an Initially Spherical Vapor Cavity in the Neighborhood of a Solid Boundary. Rep. 85-49, California Institute of Technology, Division of Engineering and Applied Science.

Strasberg, M. 1959. Onset of Ultrasonic Cavitation in Tap Water. *J. Acoust. Soc. Am.*, Vol. 31, pp. 163-176.

van Wijngaarden, L.1964. On the Collective Collapse of a Large Number of Gas Bubbles in Water. *Proceedings of the 11th International Congress on Applied Mechanics* (Springer-Verlag, Berlin), pp. 854-861.

van Wijngaarden, L. 1968. On the Equations of Motion of Mixtures of Liquid and Gas Bubbles. *Journal of Fluid Mechanics*, Vol. 33 (3), pp. 465-474.

van Wijngaarden, L. 1972. One-dimensional Flow of Liquids Containing Small Gas Bubbles. *Ann. Rev. Fluid Mech.*, Vol. 4, pp. 369-396.